Kathmandu University
Journal of Science, Engineering and Technology

Influence of groove design on the mechanical properties of AISI 1018 mild steel welded joints

Stephen Durowaye*[a], Wasiu Ayoola[a], Olalekan Hammed[b], and Ganiyu Lawal[a]

[a]Department of Metallurgical and Materials Engineering, University of Lagos, Lagos, Nigeria.
[b]Department of Mechanical Engineering, College of Technology, Yaba, Lagos, Nigeria.

Abstract

The influence of groove design on mechanical properties of AISI 1018 mild steel welded joint was studied. An 8 mm thick mild steel plate was marked out and cut to dimension of 120 × 75 × 8 mm using a portable cutting machine. Groove preparation was done for the single-V and single-beveled grooves. After proper alignment of the edges, the work pieces were welded using the Shielded Metal Arc Welding (SMAW) method with a Direct Current (D.C.) welding machine with voltage and current of 220 V and 100 A respectively. Specifically, gauge-12 (2.5 mm) stick electrodes were used for the root run while many passes (hot pass, filling and capping) were undertaken with gauge-10 (3.25 mm) electrodes because of the volume of filler metal required to fill the single-V and single beveled joints. The mechanical properties of the butt, single beveled and singe V joints were evaluated. The results showed that microstructural changes occurred in the specimens due to heat in the fusion and heat-affected zones with the appearance of ferrite, pearlite, martensite and bainite phases with grain boundaries, which confirm recrystallization. The heat-affected zone single V-joint exhibited the highest tensile strength of 442.41 MPa while fusion zone single V-joint exhibited the highest hardness of 358.9 HV. In fusion zone, the butt-joint specimen exhibited impact energy of 65.2 J/mm^2 compared to 62.37 J/mm^2 and 48.81 J/mm^2 exhibited by the single V and single beveled joints respectively. However, the heat-affected zone single V-joint exhibited the highest impact energy of 73.22 J/mm^2.

Keywords: AISI 1018 mild steel; Groove variation; Welded-joints; Mechanical properties

1. Introduction

Welding is an important fabrication process that is applied in engineering and technology. In welding, mild steel and electrodes of different grades are some of the vital materials that are used. Welding can be regarded as the joining of materials (metals or non-metals) via heat up to the appropriate temperature [1]. Various types of welding have been developed and investigated and have been found to be more beneficial than some of the other joining processes [2]. Generally, welding is very useful for effecting permanent joints in the manufacturing of automobiles, aircraft frames, railway wagons, machine frames, structural works, tanks, ship-building, etc [3]. Hence, welding is very important in engineering and technology.

The mechanical properties of joints produced after welding are influenced by some factors such as current and voltage used, applied speed, edge preparation, etc [2]. The current, voltage and applied speed are the major factors, which control the fusion, depth of penetration, heat input and shape of weld puddle while electrode polarity, angle of inclination (edge preparation) and welding technique are the secondary factors, which influence energy absorbed and melting rate of base and weld metals [2]. For instance, increase in the welding current will cause an increase in heat input and penetration with increased width of weld bead [2]. However, if the current is too high, there will be formation of a wide bead with flat and irregular shape leading to excess spatter [4].

The two main types of welding are plastic (pressure) welding and fusion (non-pressure) welding. In plastic welding, the pieces of metals to be joined are heated to a plastic state and forced together by external pressure. Example is resistance welding. In fusion welding, the materials at the joint are heated to molten state and allowed to solidify. Examples of this are gas and arc welding [3]. The equipment that are necessary for arc welding are welding generator (D.C.) or transformer (A.C.), two cables for work and electrode, electrode holder, electrode, protective shield, gloves, wire brush, chipping hammer and goggles. As regards power source, A.C. machines are less expensive but generally restricted to ferrous metals. However, D.C. equipment can be used on all metals and is generally known for better arc control [3].

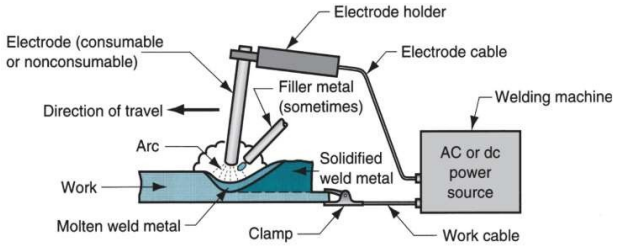

Figure 1: Diagram illustrating the arc welding equipment and process [3].

The Shielded Metal Arc Welding (SMAW) method is employed to melt and join metals by heating them with an arc established between a stick-like covered electrode and the metals. The equipment for SMAW are also simple and economical [5]. A simple diagram illustrating the arc welding equipment and process is shown in Fig. 1.

The fusion welding method, which is widely used for joining

*Corresponding author. Email: sdurowaye@unilag.edu.ng

combinations of various metals. Has its own challenges because of the formation of undesirable brittle intermetallic compounds (IMCs) at weld zone coupled with segregated phases and formation of residual stresses because of variation in the constituents of the joining metals [6]. Generally, it is very important to employ appropriate welding parameters in order to achieve a good weld because the performance of a welded joint is influenced largely by the main parameters (current, voltage and applied speed) [7].

During welding, high deposition of carbon should be avoided because it reduces ductility of the weld. It also affects negatively the weldability and impact toughness. It has been proven that materials with carbon content higher than 0.5 % in the heat-affected zone (HAZ) of weldment do exhibit high hardness resulting to brittle joint with cracking [8]. Despite these challenges, fusion-welding method is most widely used in joining of different types of ferrous alloys.

Many studies have been conducted to investigate the efficacy of fusion welding by examining the mechanical properties of welded joints of low carbon steel using the SMAW method. For instance, Talabi et al [9] studied the effect of welding parameters on the mechanical properties of welded 10 mm thick low carbon steel plate welded using the SMAW method. The results indicated that the welding parameters (current, arc voltage, welding speed and electrode thickness) had much influence on the mechanical properties of the welded specimens. Increase in voltage and current caused an increased in the hardness and decrease in yield strength, tensile strength and impact energy of the weld. Increase in the speed led to an increase in the hardness. Increased electrode diameter of enhanced the mechanical properties.

Bodude and Momohjimoh [5] investigated how increase in heat input affected the mechanical properties of low-carbon steel employing two welding methods, SMAW and oxy-acetylene welding (OAW) while using two different edge preparations with different welding parameters and mild steel electrodes. The results indicated that increased heat input enhanced the impact energy of the welded joint whereas the tensile strength and hardness decreased. Furthermore, straight edged samples exhibited lower mechanical characteristics compared to V-grooved edge samples under the same situation. The welded joints showed that using different cooling media had much influence on the resulting microstructure with different phases of ferrite and pearlite of varied ratio.

Sumardiyanto and Susilowati [10] studied the mechanical properties of API 5L low carbon steel welded joints using SMAW method with varied electrodes and current. The results revealed that variation in electrode type and current had significant effect on tensile strength, impact energy and hardness of the weld. For all types of electrodes, the tensile strength, impact energy and hardness of the welds decreased when the amount of current increased. Pathak et al [11] studied the effects of current and electrode angle on tensile strength of low carbon steel plates using SMAW. The results obtained indicated that increased current and electrode angle improved the ultimate tensile strength of the weld. In addition, variation of groove affected the mechanical properties of the samples with the single-V groove exhibiting higher impact energy than both single-beveled and double-beveled grooves. The SMAW method has proven to be effective and economical. Hence, it was used in the current study to investigate the influence of weld-joint groove variation on the mechanical properties of AISI 1018 mild steel welded joint.

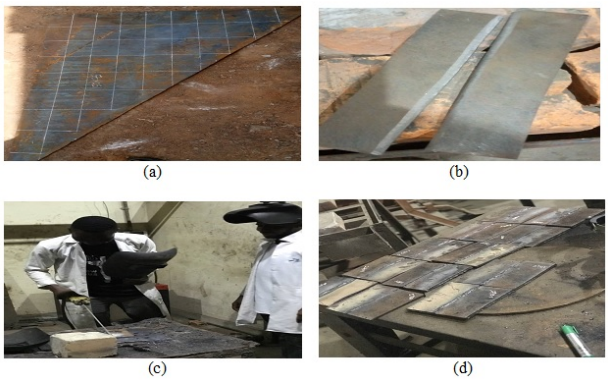

Figure 2: Snapped pictures of (a) AISI 1018 mild steel plate (b) some of the beveled mild steel plates before welding (c) welding of the plates (d) some 8 mm welded butts using a weld gap of 2 mm.

2. Materials and method

2.1. Materials and equipment

Locally sourced 8 mm thick AISI 1018 mild steel plates were employed with E6013 welding electrodes of gauge-10 (3.25 mm) and gauge-12 (2.5 mm). A Direct Current (D.C.) welding machine with a voltage and current of 220 V and 100 A respectively was used.

2.2. Specimens preparation and welding procedure

The AISI 1018 mild steel plates were marked out and cut to the specified dimension of 120 $\times$ 75 $\times$ 8 mm using a portable cutting machine. The cut plates were cleaned with acetone to remove dirt, grease and other contaminants to avoid impurities in the molten metal pool that can affect the quality of the weld-joint. Groove preparation was done for the single-V and single-beveled grooves. Specifically, oxyacetylene gas cutting was used to miter the edges of the plates in order to bring out the grooves (single V and single beveled). Thereafter, a portable grinding machine was used to achieve a perfect surface finish on each joint (butt, single V and single beveled) leaving a 2 mm gap between them (root face) for proper penetration and to reduce any chance of blowholes. After proper alignment of the edges of the work pieces, they were welded using SMAW method. A Direct Current (D.C.) welding machine with voltage and current of 220 V and 100 A respectively was used. Gauge-12 (2.5 mm) stick electrodes were used for the root run while three passes (hot, filling and capping) were undertaken with gauge-10 (3.25 mm) electrodes because of the volume of filler metal required to fill the V and single beveled joints. The work pieces were turned-over and tack welded to hold them and prevent them from warping or bending inward when the welds are finished. After welding, the slag were chipped off using chipping hammer and wire brush to clean the weld surface properly. Some of the mild steel plates before, during and after welding operation are shown in Fig. 2.

2.3. Characterization of the welded joints

The chemical composition of the as-received mild steel specimen shown in Table 1 was determined using a spectrometer. Microstructural examination was performed using an optical microscope and scanning electron microscopes (SEM). Transverse tensile test specimens were cut from welded butt joints to determine the transverse tensile strength according to ASTM E8/E8M-22 [12] standard. Each of the specimens was fitted separately to the universal tensile testing machine and load was applied at room temperature. The load and extension for the construction of stress-strain curve of each tested specimen was recorded and the Young's modulus, yield strength, ultimate tensile strength, fracture strain,

percentage elongation and percentage area of reduction of each specimen were determined using equations eqs. 1, 2, 3 and 4.

$$\sigma = \frac{F}{A} \tag{1}$$

Where
σ = Stress, F = Force and A = Area

$$A = \frac{\pi D}{4} \tag{2}$$

Where π = 3.142, D = Diameter

$$\epsilon = \frac{\Delta L}{L} \tag{3}$$

Where ΔL = change $\in$ length, L = original length

$$E = \frac{\Delta \sigma}{\Delta \epsilon} \tag{4}$$

Where E = Young's modulus, σ = stress, ϵ = strain

Hardness of specimens was determined by using a Vickers hardness tester. An indentation load of 100 gf was applied on each of the specimens in a time of 10 s in accordance with ASTM E384-11 [13] standard. Some of the specimens of size 55 × 10 × 10 mm with a V-notch of 2 mm depth at the middle for the purpose of impact test. The impact energy of the specimens was determined in accordance with ASTM E23-18 [14] standard using a Charpy impact tester. Each of the specimens was placed vertically in-between the grips of the testing machine and clamped into position. The pendulum's angle, weight, impact energy and striking velocity of 1400, 22 kg, 300 J and 5 m/s respectively were used to break the specimen.

3. Results and discussion

3.1. Microstructure

The optical micrograph of the as-received mild steel plate shown in Fig. 3 reveals the presence of ferrite matrix and the dispersion of pearlite in the microstructure. The microstructural changes in the welded joints due to heat input in the fusion and heat-affected zones are shown in the micrographs (Fig. 4 to 10). There is appearance of the ferrite, pearlite, martensite and bainite phases with grain boundaries, which confirm recrystallization. In all the micrographs of the welded joints, the microstructures were altered during the welding process such that the heat input re-distributed the phase orientation and sizes. The phases of the specimens are revealed by the Energy-dispersive Spectroscopy (EDS) spectra. Martensitic phase formation in the heat-affected zones of the specimens indicates rapid cooling of the welds during solidification [15]. In Fig. 4, 5a and 6a, there is no much change in the microstructures of the butt-joint specimens at the fusion and heat-affected zones due to lack of penetration of the weld into the butt joint [4]. The microstructures of the single beveled-joint specimens at the fusion and heat-affected zones shown in Fig. 7 and 8a also reveal the presence of ferrite, pearlite, martensite and bainite phases. The optical and SEM micrographs (Fig. 9 and 10a) of the single V-joint specimen reveal that there is recrystallization and evidence of grain growth at the fusion and heat-affected zones due to high heat input during welding. In addition, there is an increase in pearlite due to carbon deposited by the electrodes. Generally, microstructural evaluation of mild steel weldment produced could be used to evaluate the effect of welding current on the microstructural inhomogeneity of the weldment. In welding of steels, there are different solidification paths, transformation sequences, and solidification starts in most of steel welds with the formation of δ-ferrite and in most cases, accompanied by the nucleation of austenite on the δ-δ-ferrite grain boundaries [16]. The microstructure of base metal is completely different from weld metals irrespective of heat input. Fully austenitic structure with little annealing twins is observed in base microstructure. The microstructure of these weld metals contains ferrite and austenite i.e. δ-ferrite structure that could be described by primary solidification modes of weld metals [7].

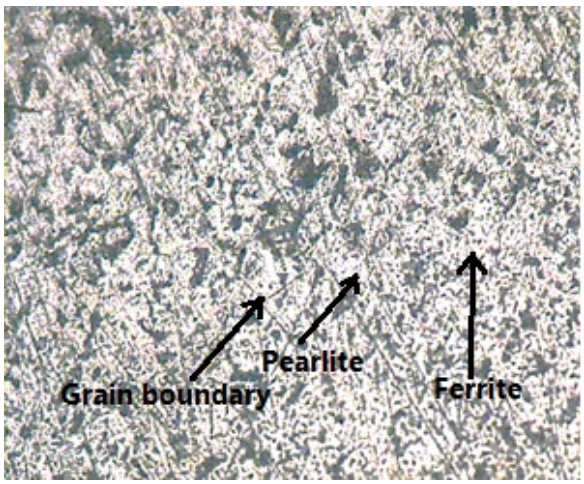

Figure 3: Optical micrograph of the as-received mild steel plate.

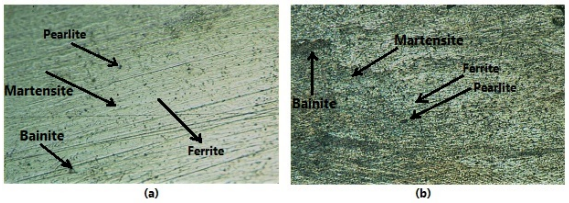

Figure 4: Optical micrographs of butt-joint specimen in (a) fusion zone (b) heat-affected zone.

3.2. Tensile strength

The fusion zone (FZ) single beveled joint exhibits tensile strength of 334.26 MPa while the single V and butt joints exhibit tensile strength of 325.89 MPa and 278.2 MPa respectively as shown in Fig. 11a. The lower tensile strength is due to lack of penetration of the weld into the single V and butt joints [4]. This could also be due to defects because the single V joint has more deposition of the electrode than the single beveled joint. As shown in Fig. 11b, the heat-affected zone single V joint exhibits the highest tensile strength of 442.41 MPa. This may be due to the even distribution of heat within the welded joint. Comparing tensile strength exhibited by specimens in the two zones, the heat-affected zone single V weld/joint exhibits the highest tensile strength (442.41 MPa) compared to the fusion zone. The lower tensile strength exhibited could be due to introduction of high heat during welding in the fusion zone, which could cause forming of defects. This agrees with the report by Talabi *et al* [9].

3.3. Hardness

In the fusion zone (FZ), the single V joint specimen exhibits the highest hardness of 358.9 HV followed by the single beveled specimen with 341.7 HV while butt specimen exhibits the lowest hardness (329.1 HV) as shown in Fig. 12a. This shows that the more the electrode has access to the root (deeper penetration), the better the joints. Similarly, in Fig. 12b, the heat-affected zone single V specimen exhibits higher hardness value than the other welded-joints. Comparing the hardness exhibited by specimens in the two

Table 1: Mild steel elemental composition.

Elements	Fe	C	Si	Mn	P	S	Cr	Ni	Cu
Weight (%)	98.3342	0.1885	0.1204	0.5456	0.101	0.086	0.0266	0.0278	0.0165

Elements	Al	Ti	V	Co	Nb	W	Sn	Ce
Weight (%)	0.0808	0.0023	0.0087	0.006	0.019	0.044	0.093	0.2996

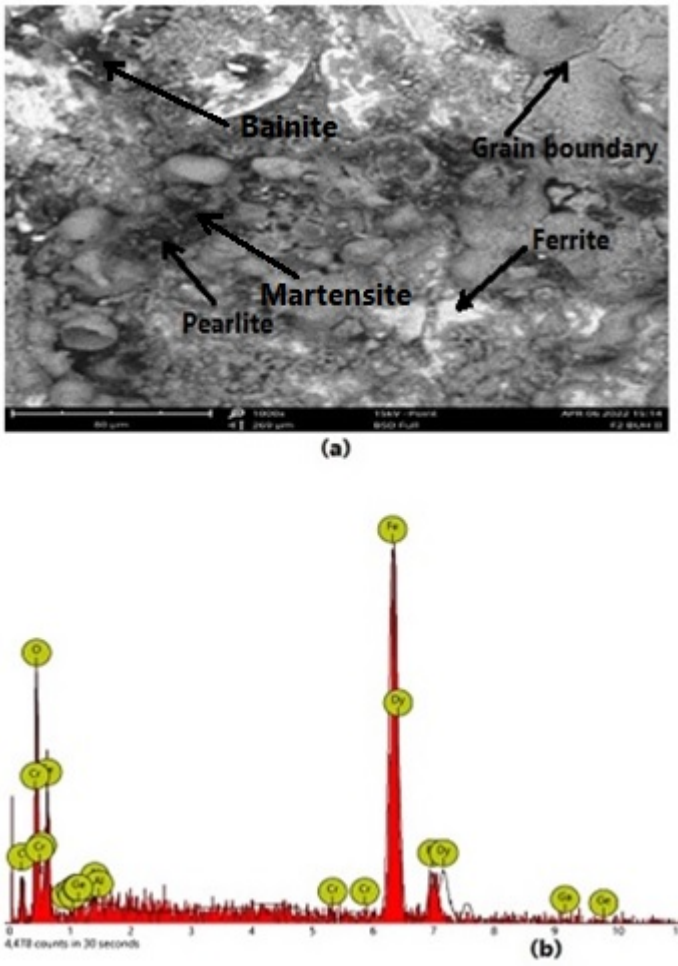

Figure 5: (a) Microstructure and (b) EDS spectrum of fusion zone butt-joint specimen.

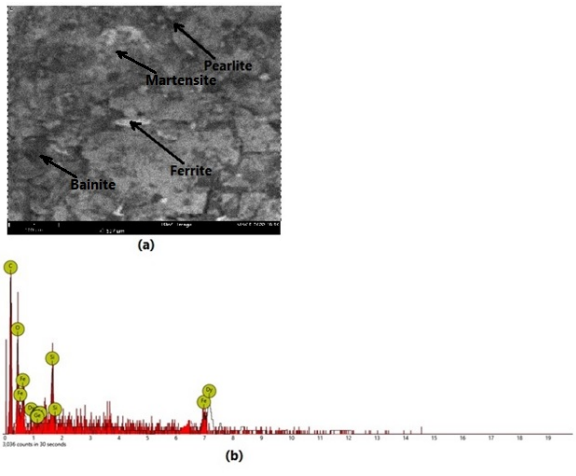

Figure 6: (a) Microstructure and (b) EDS spectrum of the heat-affected zone butt-joint specimen.

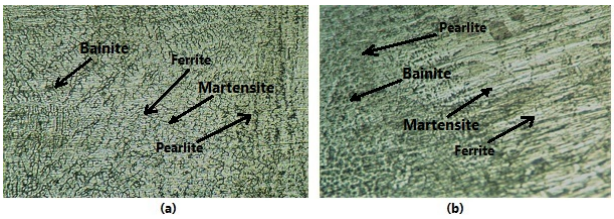

Figure 7: Optical micrographs of single beveled-joint specimen in (a) fusion (b) heat-affected zones.

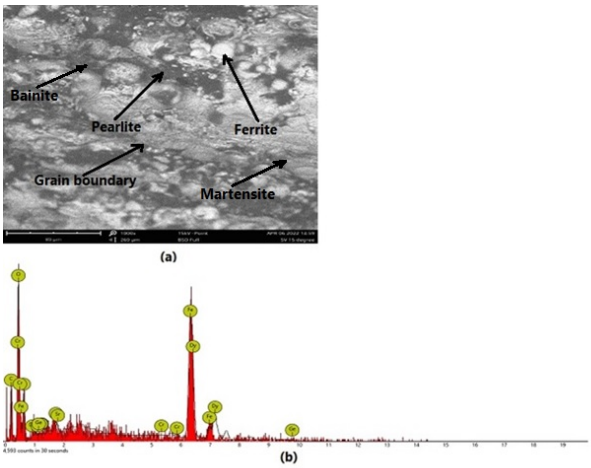

Figure 8: (a) Microstructure and (b) EDS spectrum of the fusion zone single beveled-joint specimen.

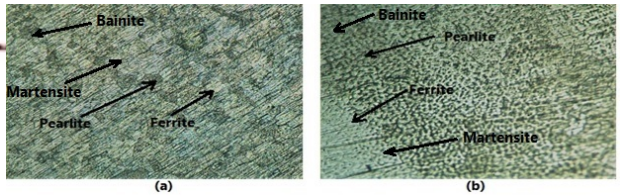

Figure 9: Optical micrographs of single V-joint specimen in (a) fusion (b) heat-affected zones.

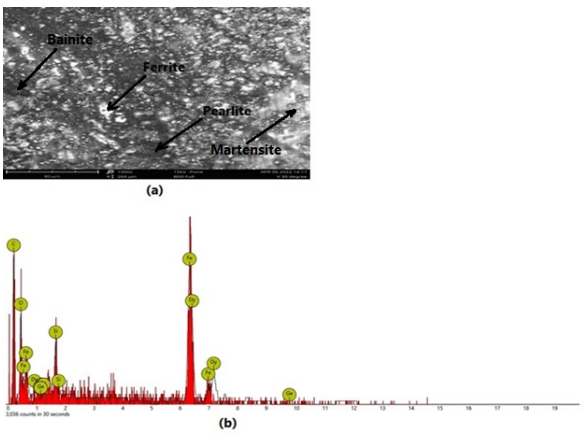

Figure 10: (a) Microstructure and (b) EDS spectrum of the fusion zone single-V joint specimen.

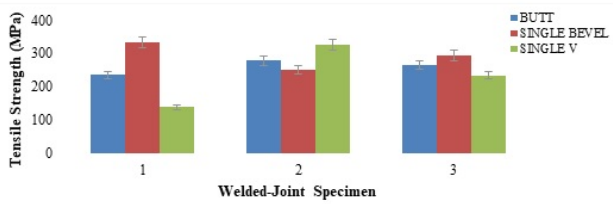

(a) Tensile strength of fusion zone welded-joint specimens.

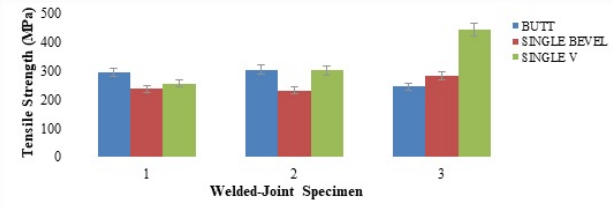

(b) Tensile strength of heat-affected zone welded-joint specimens.

Figure 11: Tensile strength.

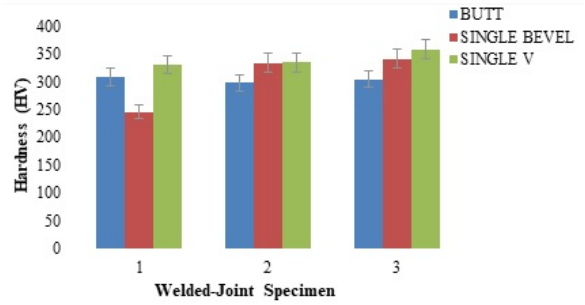

(a) Hardness of the fusion zone welded-joint specimens.

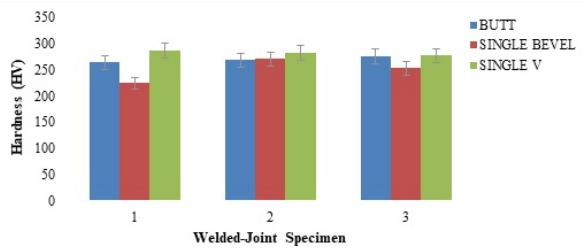

(b) Hardness of the heat-affected zone welded-joint specimens.

Figure 12: Hardness.

zones, the higher hardness exhibited is due to more carbon deposition in FZ than HAZ heat-affected zone. Generally, high hardness exhibited by the specimens in fusion and heat-affected zones may be due to martensite phase and/or carbide precipitates. This agrees with the report by Osoba *et al* [16].

3.4. Impact energy

In the fusion zone, the butt joint specimen demonstrates impact energy value of 65.2 J/mm^2 compared to 62.37 J/mm^2 and 48.81 J/mm^2 exhibited by the single V and single beveled joints respectively as presented in Fig. 13a. The lower impact energy could be due to welding slag inclusion at the joints. However, at the heat-affected zone shown in Fig. 13b, the single V joint/weld exhibits the highest impact energy of 73.22 J/mm^2. The higher impact energy value is due to the low carbon deposition during welding at the heat-affected zone. This agrees with the report by Pathak *et al* [11] where the single-V groove revealed higher in impact energy than single and double-beveled joints.

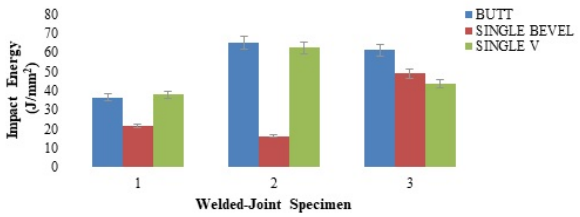

(a) Impact energy of the fusion zone welded-joint specimens.

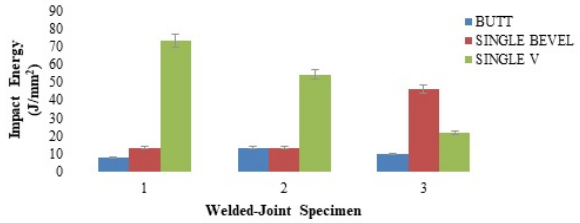

(b) Impact energy of the heat-affected zone welded-joint specimens.

Figure 13: Impact energy.

4. Conclusion

In this study, the influence of weld-joint groove variation on the mechanical properties of AISI 1018 mild steel welded joint has been investigated. From the results of investigation and discussion, the following inferences can be drawn:

1. Microstructural changes occurred in the specimens due to heat in the fusion and heat- affected zones with the appearance of the ferrite, pearlite, martensite and bainite phases with grain boundaries, which confirm recrystallization.
2. Martensitic phase formation in the heat-affected zones of the specimens indicates rapid cooling of the welds during solidification.
3. The heat-affected zone single V-joint exhibited the highest tensile strength of 442.41 MPa while fusion zone single V-joint exhibited the highest hardness of 358.9 HV.
4. In fusion zone, butt-joint specimen exhibited impact energy of 65.2 J/mm^2 compared to 62.37 J/mm^2 and 48.81 J/mm^2 exhibited by the single V and single beveled joints respectively. However, the heat-affected zone single V-joint exhibited the highest impact energy of 73.22 J/mm^2.

References

[1] Suheni, Rosidah A A, Ramadhan D P, Agustino T, Wiranata F F, Effect of welding groove and electrode variation to the tensile strength and macrostructure on 304 stainless steel and AISI 1045 dissimilar welding joint using SMAW process, *IOP Publishing, Journal of Physics: Conference Series*, 2117 (2021) 1-7.

[2] Mohanta G K & Senapati A K, The effect of welding parameters on mild steel by MMAW, IOP Conference Series: Materials Science and Engineering, 410 (2018) 1-7.

[3] Saloda M A, *Lecture Notes on Welding Technology*, Maharana Pratap University of Agriculture and Technology, Udaipur-313 001 (Rajasthan), India, 2020.

[4] OTC DAIHEN Inc., Atlanta Technical Center, 3135 Medlock Bridge Road, Norcross, GA 30071, USA. 2022.

[5] Bodude M A & Momohjimoh I, Studies on effects of welding parameters on the mechanical properties of welded low-carbon steel, *Journal of Minerals and Materials Characterization and Engineering*, 3 (2015) 142-153.

[6] Chaudhari R, Loharkar P K & Ingle A, Applications and challenges of arc welding methods in dissimilar metal joining, *IOP Conference Series: Materials Science and Engineering*, 810 012006 (2020) 1-9.

[7] Moi S C, Pal P K, Bandyopadhyay A & Rudrapati R, Effect of heat input on the mechanical and metallurgical characteristics of TIG welded joints, *Journal of Mechanical Engineering*, 16 (2) (2019) 29-40.

[8] Agarwal G, Kumar A, Richardson I M & Hermans M J M, Evaluation of solidification cracking susceptibility during laser welding in advanced high strength automotive steels, *Materials and Design,* 183 (2019) 1-12.

[9] Talabi S I, Owolabi O B, Adebisi J A & Yahaya T, Effect of welding variables on mechanical properties of low carbon steel welded joint, *Advances in Production Engineering & Management*, 9 (4) (2014) 181-186.

[10] Sumardiyanto D & Susilowati S E, Effect of welding parameters on mechanical properties of low carbon steel API 5L shielded metal arc welds, *American Journal of Materials Science*, 9 (1) (2019) 15-21.

[11] Pathak D, Singh R P, Gaur S & Balu V, Experimental investigation of effects of welding current and electrode angle on tensile strength of shielded metal arc welded low carbon steel plates, *Materials Today: Proceedings*, 26 (2) (2020) 929-931.

[12] ASTM E8/E8M-22 (2022). Standard test methods for tension testing of metallic materials. ASTM International, 100 Barr Harbor Drive, PO Box C700, West Conshohocken, PA, 19428-2959, USA.

[13] ASTM E384-11 (2017). Standard test methods for Vickers hardness and Knoop hardness of metallic materials. ASTM International, 100 Barr Harbor Drive, PO Box C700, West Conshohocken, PA, 19428-2959, USA.

[14] ASTM E23-18 (2018). Standard test methods for notched bar impact testing of metallic materials. ASTM International, 100 Barr Harbor Drive, PO Box C700, West Conshohocken, PA, 19428-2959, USA.

[15] Nhung L T, Khanh P M, Hai L M & Nam N D, The relationship between continuous cooling rate and microstructure on the heat affected zone (HAZ) of the dissimilar weld between carbon steel and austenitic stainless steel, *Acta Metallurgical Slovaca*, 23 (4) (2017) 363- 370.

[16] Osoba L O, Ayoola W A, Adegbuji Q A & Ajibade O A, Influence of heat inputs on weld profiles and mechanical properties of carbon and stainless steel, *Nigerian Journal of Technological Development*, 18 (2) (2021) 135-143.